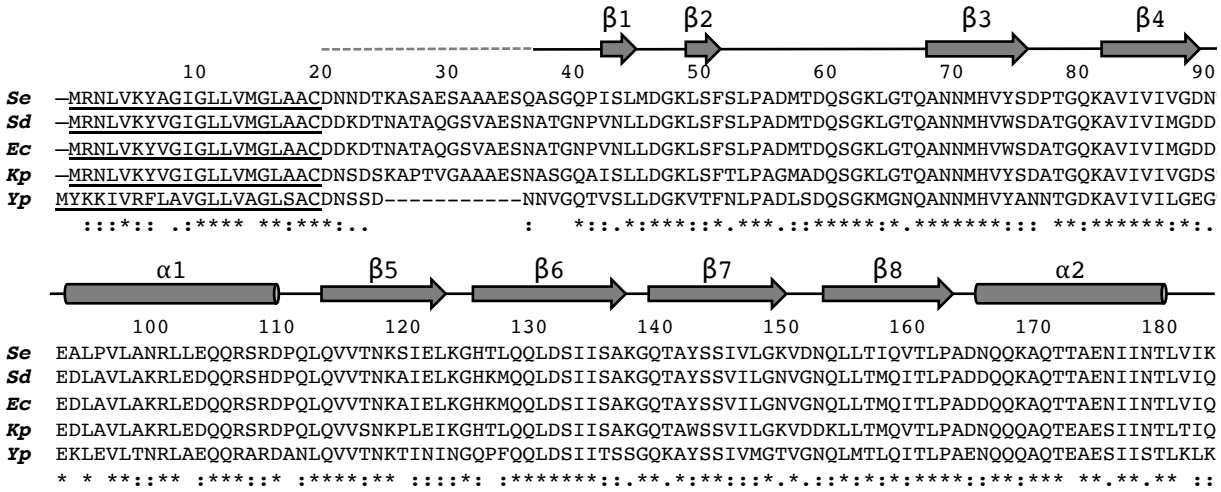

Supplementary Figure 1. Multiple sequence alignment of DcrB proteins from enterobacterial pathogens. The secondary structure that was observed in the structure of DcrBΔ37 is indicated over the multiple sequence alignment. The multiple sequence alignment includes DcrB sequences from *Salmonella enterica* serovar Typhimurium (*Se*), *Shigella dysenteriae* (*Sd*), *Escherichia coli* (*Ec*), *Klebsiella pneumoniae* (*Kp*), and *Yersinia pestis* (*Yp*). The lipoprotein signal sequence is underlined. The dashed gray line indicates the portion of purified SeMet DcrBΔ20 protein that was not observed in electron density maps. Solid black lines correspond to regions of DcrBΔ37 that were observed in electron density maps but were not part of α-helices or β-strands. Symbols underneath each aligned position indicate residues that are completely conserved (*), residues that are strongly conserved (:), and residues that are weakly conserved (.) (Chenna et al., 2003)

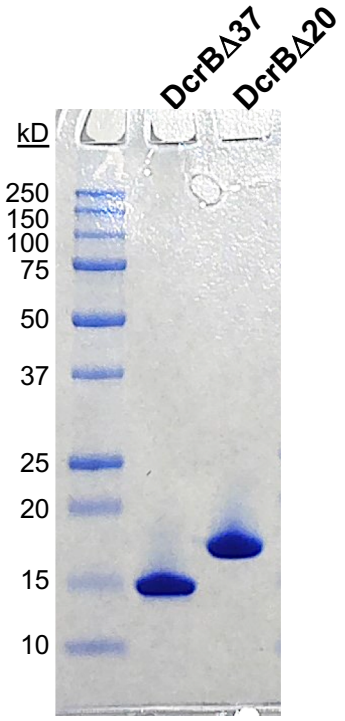

Supplementary Figure 2. Analysis of 20 µg of purified DcrBΔ20 (18.6 kD) or 20 µg of DcrBΔ37 (16.9 kD) by SDS-polyacrylamide gel electrophoresis followed by Coomassie staining.

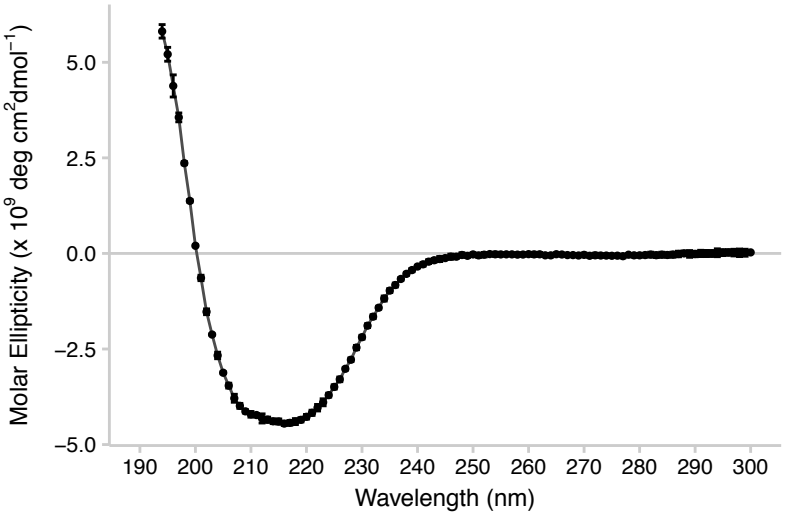

Supplementary Figure 3. DcrB consists primarily of β-sheet in solution. Molar ellipticity values from a circular dichroism wavelength scan of DcrBΔ37 are plotted as the mean of 3 independent experiments, and error bars represent standard deviations.

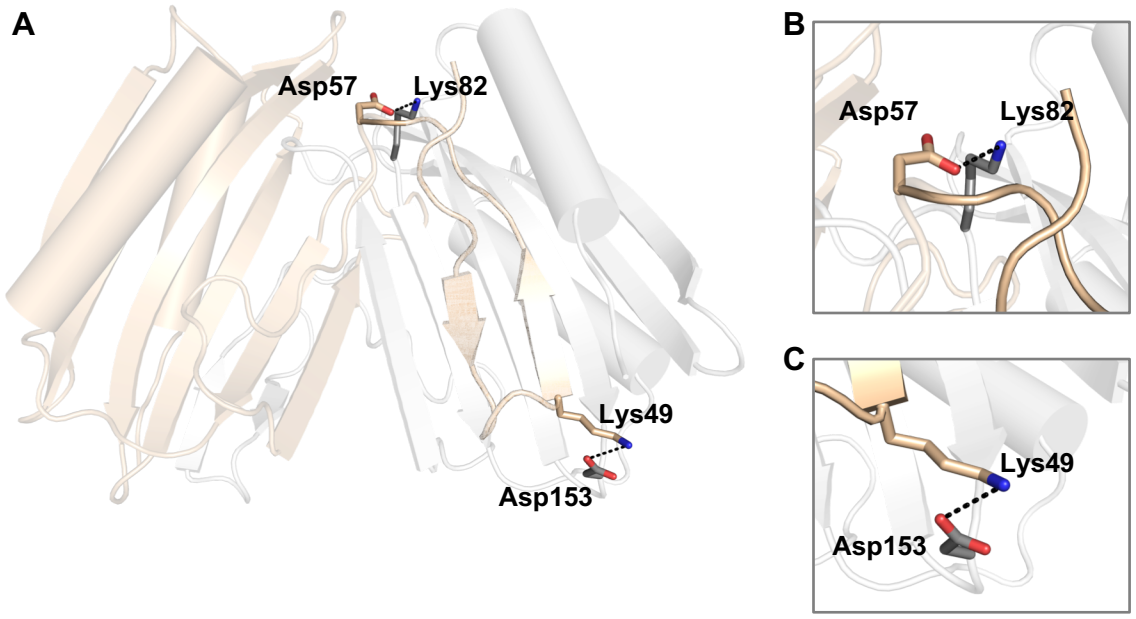

Supplementary Figure 4. Salt bridge interactions in the domain-swapped dimer of DcrBΔ37. A) The two salt bridges are depicted between the β-hairpin of one DcrBΔ37 monomer (wheat) and the other DcrBΔ37 monomer (light gray). The side chains of residues involved in these salt bridges are depicted as sticks, with oxygen atoms in red, nitrogen atoms in blue, and carbon atoms in either wheat (one monomer) or gray (second monomer). B) Zoomed views of the Asp57–Lys82 salt bridge (B) and Lys49–Asp153 salt bridge (C), colored the same as described in panel A. The black dashed line indicates the electrostatic interaction between the side chains.

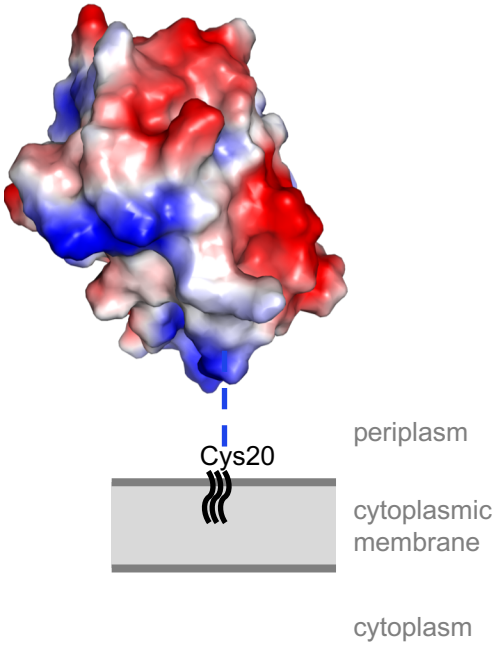

Supplementary Figure 5. Predicted electrostatic charge of DcrB relative to the cytoplasmic membrane. The DcrB monomer is colored based on the calculated surface electrostatic charge, where red represents regions of negative charge and blue represents regions of positive charge. The dotted lines represent the unstructured region, corresponding to amino acids 21–37, that connect the lipid-modified Cys20 to the structured domain of DcrB.

Supplementary Table 1. Oligonucleotide primers used in this study

Primer name	Sequence (5' to 3')
JM012	TATACATATGCATCATCATCATCATCATGCAGATAACAACGATACAAAAGC
JM013	CCCAAGCTTACTTAATAACCAACGTATTGATGATGTTTTCAGCCGTGGTTT
T7-promoter	TAATACGACTCACTATAGGG
T7-terminator	GCTAGTTATTGCTCAGCGG

Supplementary Table 2. Bacterial strains and plasmids used in this study

Strain or plasmid	Description	Reference or Source
Salmonella enterica		
14028s	wild-type	(Fields et al., 1986)
Escherichia coli		
DH5α	F–*sup*E44 Δ*lac*U169 (ϕ80 *lacZ*ΔM15) *hsd*R17 *rec*A1 *end*A1 *gyr*A96 *thi*-1 *rel*A1	(Hanahan, 1983)
C41(DE3)	F^- *ompT hsdSB* (rB^- mB^-) *gal dcm* (*λ* DE3) *λ DE3 = λ sBamHIo ΔEcoRI-B int::(lacI::PlacUV5::T7 gene1) i21 Δnin5*	Lucigen
JW0374–1	F^-, Δ *(araD-araB)567*, *ΔlacZ4787*(::rrnB-3), Δ*phoA748::kan*, λ^-, *rph-1*, *Δ(rhaD-rhaB)568*, *hsdR514*	Yale Coli Genetic Stock Center
JM273	C41(DE3) Δ*phoA748::kan*	This work
JM280	C41(DE3) Δ*phoA748::kan* / pET-22b-His_6*dcrBΔ20*	This work
JM296	C41(DE3) Δ*phoA748::kan* / pET-22b-His_6*dcrBΔ37*	
Plasmids		
pBR322	rep_{pMB1} Amp^R Tet^R	New England Biolabs
pBR322-*dcrB*	rep_{pMB1} Amp^R Tet^S	This work
pET-22b(+)	rep_{pMB1} Amp^R *lacI* P_{T7}	Novagen
pET-22b-His_6*dcrBΔ20*	rep_{pMB1} Amp^R *lacI* P_{T7}-His_6-*dcrBΔ20*	This work
pET-22b-His_6*dcrBΔ37*	rep_{pMB1} Amp^R *lacI* P_{T7}-His_6-*dcrBΔ37*	This work, Genscript

Supplementary Table 3. X-ray diffraction data collection statistics for SeMet DcrBΔ20

	SeMet DcrBΔ20
Data Collection	
Beamline	21-ID-D, LS-CAT, APS
Wavelength, Å	0.97895
Resolution range (high resolution bin), Å	95.71–2.30 (2.33–2.30)
Space Group	P 21 21 2
Unit Cell (a, b, c (Å))	82.44, 191.41, 41.06
(α, β, γ (°))	90, 90, 90
Completeness, %	98.6 (92.0)
Total Reflections	263,245 (11,921)
Unique Reflections	29,643 (1,350)
Redundancy	8.9 (8.8)
<I/σI>	11.5 (4.5)
R_{merge}[†], %	16.4 (77.7)
Phasing	
Figure of Merit	0.4358

[†] $R_{merge} = \Sigma\Sigma_j|I_j - \langle I \rangle|\Sigma I_j$, where I_j is the intensity measurement for reflection j and $\langle I \rangle$ is the mean intensity for multiply recorded reflections.

Supplementary Table 4. Determination of solution molecular weight (MW) of DcrBΔ20 by size-exclusion chromatography multi-angle light scattering[1]

Protein concentration	SEC-MALS MW (kD)	Range of SEC-MALS MW across eluted peak (kD)	Calculated monomeric MW	Mono-disperse peak
1.3 mg/mL	19 ± 1	18.5-21.0	18.6 kD	Yes

[1]This analysis was carried out by the W.M. Keck Foundation Biotechnology Resource Laboratory at Yale University.

Supplementary References

Chenna, R., Sugawara, H., Koike, T., Lopez, R., Gibson, T.J., Higgins, D.G., Thompson, J.D., 2003. Multiple sequence alignment with the Clustal series of programs. Nucleic Acids Res. 31, 3497–500.

Fields, P.I., Swanson, R. V, Haidaris, C.G., Heffron, F., 1986. Mutants of *Salmonella typhimurium* that cannot survive within the macrophage are avirulent. Proc. Natl. Acad. Sci. 83, 5189–5193. https://doi.org/10.1073/pnas.83.14.5189

Hanahan, D., 1983. Studies on transformation of *Escherichia coli* with plasmids. J. Mol. Biol. 166, 557–580. https://doi.org/10.1016/S0022-2836(83)80284-8